



## RESEARCH ARTICLE

# Imaging-based pregenetic screening for *NOTCH3* p.R544C mutation in ischemic stroke in Taiwan

Yu-Wen Cheng<sup>1,2</sup> , Chih-Hao Chen<sup>3</sup> , Chaur-Jong Hu<sup>4</sup>, Hung-Yi Chiou<sup>5</sup>, Sung-Chun Tang<sup>3</sup>  & Jiann-Shing Jeng<sup>3</sup><sup>1</sup>Department of Neurology, National Taiwan University Hospital, Hsin-Chu Branch, Hsin-Chu, Taiwan<sup>2</sup>Graduate Institute of Clinical Medicine, College of Medicine, National Taiwan University, Taipei, Taiwan<sup>3</sup>Stroke Center and Department of Neurology, National Taiwan University Hospital, Taipei, Taiwan<sup>4</sup>Department of Neurology, Taipei Medical University Hospital and Shuang Ho Hospital, Taipei, Taiwan<sup>5</sup>School of Public Health, College of Public Health, Taipei Medical University, Taipei, Taiwan

## Correspondence

Sung-Chun Tang, Stroke Center and Department of Neurology, National Taiwan University Hospital, No. 7 Chung-Shan South Road, Taipei 10055, Taiwan. Tel: 886-2-23562144; Fax: 886-2-23418395; E-mail: sctang@ntuh.gov.tw

Received: 5 June 2020; Revised: 8 August 2020; Accepted: 24 August 2020

*Annals of Clinical and Translational Neurology* 2020; 7(10): 1951–1961

doi: 10.1002/acn3.51191

## Abstract

**Objective:** To develop an easily applicable screening score to guide *NOTCH3* p.R544C genetic testing for patients who presented with acute ischemic cerebrovascular events in Taiwan. **Methods:** 1734 patients who presented with ischemic cerebrovascular events were enrolled from the Formosa Stroke Genetic Consortium stroke registry and were screened for the *NOTCH3* p.R544C mutation. Clinical and MRI characteristics of *NOTCH3* p.R544C mutation carriers (n = 36) and a subset of noncarriers (n = 673) were tested in a logistic regression model to identify key features associated with the *NOTCH3* p.R544C carrier status. Variables and their odds ratios in the regression model were used to develop the R544C screening score to predict positive *NOTCH3* p.R544C test results. **Results:** We constructed the R544C screening score using five clinical and imaging characteristics, including stroke onset before 50 years of age, the small vessel occlusion subtype, a family history of stroke/TIA in siblings, external capsule involvement, and advanced deep white matter hyperintensity. The area under the ROC curve of the screening score was 0.867 (95% CI = 0.810–0.924). The sensitivity, specificity, positive predictive value, negative predictive value and accuracy were 0.75, 0.88, 0.13, 0.99, and 0.88, respectively, for a cut-off score of 5 points. In addition, the R544C screening score was validated in another cohort composed of 235 stroke patients with comparable performance (area under the ROC curve = 0.957, 95% CI = 0.916–0.997). **Interpretations:** For Taiwanese patients presenting with acute ischemic cerebrovascular events, the R544C screening score is easily applicable and can efficiently select high-risk patients for *NOTCH3* p.R544C mutation test.

## Introduction

Cerebral autosomal dominant arteriopathy with subcortical infarcts and leukoencephalopathy (CADASIL) is the most prevalent monogenetic disease that causes cerebral small vessel disease and stroke. It is caused by mutations in the *NOTCH3* gene on chromosome 19p13.<sup>1</sup> There are more than 200 documented pathogenic mutations, most of which are alternations of the number of cysteine residues in the conserved epidermal growth factor-like repeat (EGFR) domains.<sup>2,3</sup> Across different ethnic groups, there are considerable variations in the *NOTCH3* mutation

frequency and the dominant mutation type. In East Asia, the frequency of EGFR cysteine-altering *NOTCH3* mutations has been estimated to be 9.0/1000, which is much higher than that in European, Latino, and African American individuals.<sup>2</sup>

In Taiwan, 70% of CADASIL cases are caused by the *NOTCH3* p.R544C mutation at EGFR domain 13/14.<sup>4</sup> Recent studies suggested that *NOTCH3* p.R544C mutation is an important, though often underdiagnosed, risk factor for ischemic stroke in Taiwan.<sup>5,6</sup> Tang *et al.* investigated the prevalence of the *NOTCH3* p.R544C mutation in Taiwanese stroke patients from data extracted from the

Formosa Stroke Genetics Consortium (FSGC).<sup>5</sup> The prevalence of the *NOTCH3* p.R544C mutation is 2.4% in patients who presented with acute ischemic stroke and up to 5.6% in the small vessel occlusion (SVO) subtype of ischemic stroke. Concordant with the above findings, Liao *et al.* reported the presence of the *NOTCH3* p.R544C mutation in 0.9% of Taiwanese healthy controls, 2.1% of patients with ischemic stroke, and 6.5% of patients with the SVO subtype of ischemic stroke.<sup>6</sup> In addition to those from Taiwan, studies on individuals from Jeju Island of South Korea<sup>7</sup> and Fujian province in China<sup>8</sup> have indicated that the p.R544C mutation accounts for the majority of their CADASIL cases. Compared with *NOTCH3* mutations located at EGFR domains 1-6, the p.R544C mutation seemed to be clinically “milder,” having a later age of onset, less frequent white matter lesions involving the anterior temporal pole, and less frequent migraine.<sup>2,4,8</sup>

Because of its comparatively milder phenotype, the *NOTCH3* p.R544C mutation is often underdiagnosed in clinical settings. In addition, the later age of onset opens the possibility that early intervention, such as vascular risk factor modification, may be able to modify the disease course. Therefore, targeted genetic testing for the *NOTCH3* p.R544C mutation may help identify CADASIL cases at an early stage and lead to further investigation for disease-modifying interventions. By combining imaging and clinical characteristics, we aimed to develop an easily applicable screening score that could lead to further *NOTCH3* p.R544C mutation screening for Taiwanese patients who present with acute ischemic stroke.

## Methods

### Study design and participants

The FSGC is a prospective, multicenter stroke registry that recruits stroke patients in Taiwan.<sup>9</sup> The R544C screening score was developed from 1734 patients with ischemic stroke or transient ischemic attack (TIA) enrolled from the FSGC and validated by a second group of 235 patients enrolled from the stroke center of National Taiwan University Hospital. Subjects who presented with acute ischemic stroke or TIA within 10 days of onset were enrolled from the FSGC during April 2005 to July 2015 and screened for the *NOTCH3* p.R544C mutation as described previously.<sup>5</sup> TIA was defined as a transient focal neurologic deficit of ischemic origin that resolved within 24 hours.<sup>10</sup> Acute ischemic stroke was defined as the acute onset of a neurological deficit with signs or symptoms persisting longer than 24 hours with or without acute ischemic lesion(s) on brain CT or with

acute ischemic diffusion-weighted imaging lesion(s) on MRI that corresponded to the clinical presentations.<sup>10</sup>

Enrolled subjects received a structured questionnaire for clinical characteristics and blood sampling. The stroke subtypes were classified according to the Trial of Org 10172 in Acute Stroke Treatment (TOAST) criteria.<sup>11</sup> Among patients harboring the *NOTCH3* p.R544C mutation (N = 41), 36 had brain MRI for the index ischemic event available and were included for imaging analysis. Among those subjects who did not harbor the *NOTCH3* p.R544C mutation, the subgroup of subjects (n = 673) recruited from two medical centers, National Taiwan University Hospital and Shuang Ho Hospital, were selected for imaging analysis. The validation cohort was composed of 235 stroke patients enrolled from the stroke center of the National Taiwan University Hospital, using the same inclusion and exclusion criteria as that for the FSGC, but different recruiting periods from the derivation group.

### Brain MRI acquisition and visual rating for imaging characteristics

Magnetic resonance imaging (MRI) of the brain was performed on a 1.5T MRI scanner. The scanning protocol included axial T2-weighted-fluid-attenuated inversion recovery (T2-FLAIR), fast spin-echo T2-weighted sequences, and a coronal T1-weighted image (T1WI) or a 3D T1WI. Imaging characteristics, including infarct size, infarct location, extent of white matter hyperintensity (WMH), white matter lesions involving the anterior temporal pole and external capsule, and the severity of mesial temporal atrophy (MTA), were evaluated with semiquantitative and qualitative methods. The infarct size was classified into three groups: less than 1.5 cm, 1.5 to 4.0 cm, or larger than 4.0 cm in the largest diameter. The infarct location was classified into eight areas: cortical, white matter or subcortical, basal ganglia, thalamus, brainstem, cerebellum, borderzone, and multiple infarctions. The extent of WMH in the periventricular white matter (PVWM) and deep white matter (DWM) were rated separately using the Fazekas score.<sup>12</sup> The WMH from the T2-FLAIR series of brain MR images was rated from 0 to 3 on an axial view, with a higher score indicating a more extensive WMH. Each side of the hemisphere was rated separately, and the average score of the two sides was used to represent the extent of WMH for each subject. White matter lesions involving the anterior temporal pole and the external capsule were coded as dichotomous variables. The severity of MTA was rated on a coronal view of the T1WI of the brain MRI scan using the scoring system proposed by Scheltens *et al.*<sup>13</sup> Each side of the medial temporal lobe and the hippocampus was scored from 0 to

4. A higher MTA score indicated more advanced medial temporal lobe atrophy. The average score of the two hemispheres was used to represent the severity of MTA for each subject.

To calculate the interrater reliability of visual scoring, 30 MRI scans were rated independently by two experienced neurologists (SCT and YWC). Cohen's kappa and the linearly weighted kappa were calculated for binominal and ordinal variables, respectively. There was strong interrater agreement for white matter lesions involving the anterior temporal pole (kappa = 0.805, 95% CI = 0.593-1.017), lesions involving the external capsule (kappa = 0.860, 95% CI = 0.707-1.013), and WMH of the DWM (weighted kappa = 0.825, 95% CI = 0.730-0.920). The interrater agreement for WMH of the PVWM was moderate (weighted kappa = 0.677, 95% CI = 0.539-0.816).

### Statistical analysis

To compare the demographic and imaging characteristics between groups, the independent Student's t-test or the Mann-Whitney U test was used for continuous variables, and the Chi-square or Fisher's exact test was used for

categorical variables. To identify key predictors for subjects harboring the *NOTCH3* p.R544C mutation, a forward stepwise multivariable logistic regression model was applied to estimate the odds ratio (OR) and 95% confidence interval (CI). Clinical and imaging characteristics that significantly differed between the *NOTCH3* p.R544C mutation carriers and noncarriers were selected as independent variables for the regression model. A *P*-value < 0.05 for entry and a *P*-value > 0.10 for removal from the model were set for the stepwise selection method. The discriminative ability of the prediction models was tested by calculating the area under the receiver operating characteristic (ROC) curve, and the calibration was calculated using the Hosmer-Lemeshow goodness-of-fit test. Based on the estimated odds ratio for each clinical and imaging characteristic, we developed a simplified R544C screening score to predict a positive *NOTCH3* p.R544C mutation identification. For each scale, the sensitivity, specificity, positive predictive value (PPV), negative predictive value (NPV), and Youden's J statistic were calculated to determine the optimal cutoff point to predict a positive *NOTCH3* p.R544C mutation. The area under the ROC curve, PPV, and NPV were calculated in the validation cohort to test the performance of the

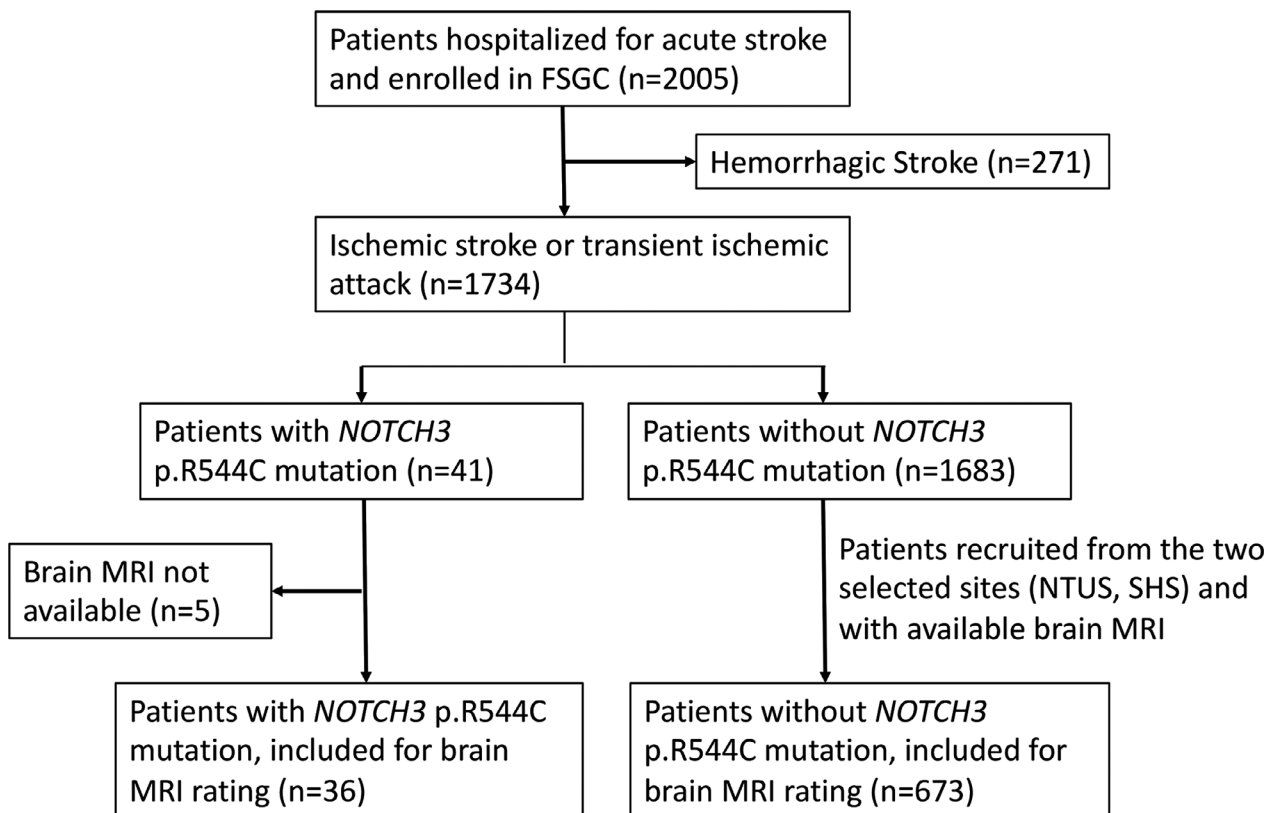


**Figure 1.** Flowchart of participants recruitment.

R544C screening score. The clinical usefulness of the final prediction score was demonstrated using decision curve analysis.<sup>14,15</sup> Data were analyzed using the statistical software SPSS for Windows, version 25.0, and R version 4.0.2 (for decision curve analysis).

### Standard protocol approvals, registrations, and patient consents

The study was approved by the local ethical committees of the participating hospitals. All investigations were conducted according to the principles expressed in the Declaration of Helsinki. All the participants or their proxies provided written informed consent before enrollment.

## Results

The study flowchart is shown in (Fig. 1). As shown in (Table 1), the SVO stroke subtype (53.7% vs 27.8%,  $P < 0.0005$ ) and a family history of stroke or TIA in siblings (25.9% vs 9.8%,  $P = 0.015$ ) were more frequent in subjects harboring a *NOTCH3* p.R544C mutation. Importantly, the distributions of age, gender, and stroke severity were similar between the subset of subjects enrolled for

imaging analysis and the source population of subjects without the *NOTCH3* p.R544C mutation. Among *NOTCH3* p.R544C noncarriers, the prevalence of vascular risk factors was similar, except for a more frequent history of TIA (5.3% vs 3.6%,  $P = 0.003$ ) and hypertension (79.2% vs 75.4%,  $P = 0.004$ ) and a more frequent family history of parental stroke (29.1% vs 26.3%,  $P = 0.041$ ) in the subset of subjects enrolled for imaging analysis. The frequency of the SVO stroke subtype was slightly higher among the subset of subjects enrolled for imaging analysis (30.8% vs 27.8%,  $P = 0.025$ ).

### MRI characteristics between p.R544C mutation carriers and noncarriers

The comparison of imaging characteristics between the *NOTCH3* p.R544C mutation carriers and noncarriers are shown in (Table 2). Subjects harboring the *NOTCH3* p.R544C mutation more frequently had a stroke located in the white matter (55.6% vs 14.3%), had more extensive WMH in both the PVWM (Fazekas score 2.58 vs 1.53,  $P < 0.0005$ ) and DWM (Fazekas score 2.25 vs 1.17,  $P < 0.0005$ ), had more advanced mesial temporal atrophy (Scheltens scale 1.46 vs 1.08,  $P = 0.034$ ), and more

**Table 1.** Clinical characteristics between *NOTCH3* p.R544C mutation carriers and non-carriers.

Clinical characteristics	p.R544C (+), N = 41	p.R544C (-), N = 1683	p.R544C(-) with MRI rating, N = 673	P-value <sup>†</sup>
Age, y	58.3 ± 10.0	61.9 ± 13.6	61.4 ± 14.5	0.100
Gender, male %	63.4	70.2	69.4	0.351
NIHSS at presentation	4.6 ± 3.8	6.9 ± 6.6	6.9 ± 6.4	0.001**
TOAST classification, %				0.003**
LAA	26.8	34.4	31.4	
SVO	53.7	27.8	30.8	<0.0005**
CE	4.9	14.6	13.7	
SE	0.0	8.0	12.6	
UD	14.6	15.3	11.6	
Vascular risk factors, %				
Previous stroke	26.8	21.8	19.6	0.442
Previous TIA	10.3	3.6	5.3	0.055
Diabetes mellitus	29.3	38.9	37.8	0.211
Hypertension	73.2	75.4	79.2	0.742
Dyslipidemia	46.2	48.4	45.7	0.783
Smoking	52.9	48.8	46.0	0.632
Family history, %				
Stroke/TIA in parents	28.0	26.3	29.1	0.850
Stroke/TIA in siblings	25.9	9.8	10.4	0.015*

Data were presented by mean ± SD or percentage (%).

Note: p.R544C (+), *NOTCH3* p.R544C mutation carriers; p.R544C (-), *NOTCH3* p.R544C mutation noncarriers;

CE, cardioembolism; LAA, large-artery atherosclerosis; NIHSS, NIH Stroke Scale; SE, stroke of other determined etiology; SVO, small-artery occlusion; TIA, transient ischemic attack; TOAST, Trial of Org 10172 in Acute Stroke Treatment; UD, stroke of undetermined etiology.

\* $P < 0.05$ , \*\* $P < 0.01$ .

<sup>†</sup>P-value of the clinical characteristics was derived from the comparison between p.R544C(+) (n = 41) and p.R544C(-) (n = 1683) subjects in the FSGC stroke registry.

**Table 2.** Imaging characteristics between *NOTCH3* p.R544C mutation carriers and noncarriers.

Imaging characteristics	p.R544c (+), N = 36	p.R544C(-), N = 673	P-value <sup>†</sup>
Stroke location, No. (%)			<0.0005**
Cortical	1 (2.8)	139 (20.7)	
White matter	20 (55.6)	96 (14.3)	
Basal ganglia	1 (2.8)	60 (8.9)	
Thalamus	2 (5.6)	48 (7.1)	
Brainstem	5 (13.9)	105 (15.6)	
Cerebellum	2 (5.6)	43 (6.4)	
Borderzone	0 (0.0)	41 (6.1)	
Multiple	3 (8.3)	105 (15.6)	
Stroke size, No. (%)			0.401
<1.5 cm	23 (63.9)	335 (49.8)	
1.5-4.0 cm	9 (25)	221 (32.8)	
>4.0 cm	3 (8.3)	97 (14.4)	
PVWM Fazekas score	2.58 ± 0.69	1.53 ± 1.04	<0.0005**
DWM Fazekas score	2.25 ± 0.93	1.17 ± 0.89	<0.0005**
MTA Scheltens scale	1.46 ± 1.04	1.08 ± 0.92	0.034*
Anterior temporal involvement, No. (%)	8 (22.2)	24 (3.6)	<0.0005**
External capsule involvement, No. (%)	25 (69.4)	96 (14.3)	<0.0005**

Data were presented by mean ± SD or count (percentage).

Note: p.R544C (+), *NOTCH3* p.R544C mutation carriers; p.R544C (-), *NOTCH3* p.R544C mutation noncarriers.

DWM, deep white matter; MTA, mesial temporal atrophy; PVWM, periventricular white matter.

\* $P < 0.05$ , \*\* $P < 0.01$ .

<sup>†</sup>P-value of the imaging characteristics was derived from the comparison between p.R544C(+) ( $n = 36$ ) and the subset of p.R544C(-) ( $n = 673$ ) subjects who received brain MRI rating.

frequently had white matter lesions involving the external capsule (69.4% vs 14.3%,  $P < 0.0005$ ) or the anterior temporal pole (22.2% vs 3.6%,  $P < 0.0005$ ). The infarct size did not differ between the two groups.

The imaging characteristics in different age groups are shown in (Fig. 2). In addition to its association with the carrier status of the *NOTCH3* p.R544C mutation, the extent of WMH increased with advanced age (Fig. 2A). Among the *NOTCH3* p.R544C carriers, the Fazekas score in either the PVWM or DWM reached the maximum score (3.0) for most of the subjects aged more than 60 years. Additionally, the frequency of white matter lesions involving the anterior temporal pole increased with advanced age among the *NOTCH3* p.R544C mutation carriers, whereas it remained less than 5% among the noncarriers (Fig. 2C). Regardless of age, the frequency of white matter lesions involving the external capsule was much higher among the *NOTCH3* p.R544C carriers than the noncarriers (Fig. 2D). MTA was more advanced in the *NOTCH3* p.R544C mutation carriers in all age groups

(Fig. 2B). In addition, MTA was associated with advanced age in both the *NOTCH3* p.R544C mutation carriers and noncarriers.

### Development and performance of the *NOTCH3* p.R544C mutation risk score

(Table 3) shows three models of multiple logistic regression analysis for the clinical and imaging characteristics associated with a positive *NOTCH3* p.R544C mutation status. Model 1 was constructed using the stepwise logistic regression method. A younger age of stroke (OR = 0.92, 95% CI = 0.88-0.97), the SVO stroke subtype (OR = 3.01, 95% CI = 1.19-7.64), a family history of stroke or TIA in siblings (OR = 3.42, 95% CI = 1.07-10.95), white matter lesions involving the external capsule (OR = 4.18, 95% CI = 1.33-13.13), and a higher DWM Fazekas score (OR = 4.35, 95% CI = 2.14-8.86) were identified as key factors associated with the *NOTCH3* p.R544C mutation status (Table 3, model 1). The interaction term between DWM Fazekas score and age did not reach statistical significance ( $P = 0.263$ ), thus was not included in Model 1. To simplify the scoring system, we classified age of stroke into four strata and the DWM Fazekas score into two groups (Table 3, model 2). An age of stroke younger than 50 years was significantly associated with the *NOTCH3* p.R544C mutation carrier status. The cutoff of the DWM Fazekas score was determined based on the distribution of the score in different age groups (Fig. 2A). The significant DWM Fazekas score for age was defined as an average Fazekas score > 1 for subjects at or younger than 60 years and an average Fazekas score > 2 for subjects older than 60 years. Model 3 was simplified from model 2 and used only five dichotomous variables to predict the p.R544C mutation status. The performance of model 3, measured by the area under the ROC curve, was comparable to that of models 1 and 2 (Fig 3A,C). The areas under the ROC curve for models 1, 2, and 3 were 0.920, 0.902, and 0.900, respectively.

Based on the estimated odds ratio in model 3, we developed the R544C screening score. The scoring items are shown in (Table 4). The sum of the scores ranged 0 to 8, with a higher score indicating a greater likelihood of a positive *NOTCH3* p.R544C mutation test result. The ROC curve for the R544C screening score is shown in (Fig. 3). The area under the ROC curve was 0.867 (95% CI = 0.840-0.892,  $P < 0.01$ ), indicating good performance. To be applied as a screening tool that could lead to further genetic testing, adequate sensitivity is required. On the other hand, adequate specificity is also important for the screening score to be applied efficiently in the clinical setting. A cutoff score of 5 was chosen to maximize Youden's J statistic, and the associated sensitivity,

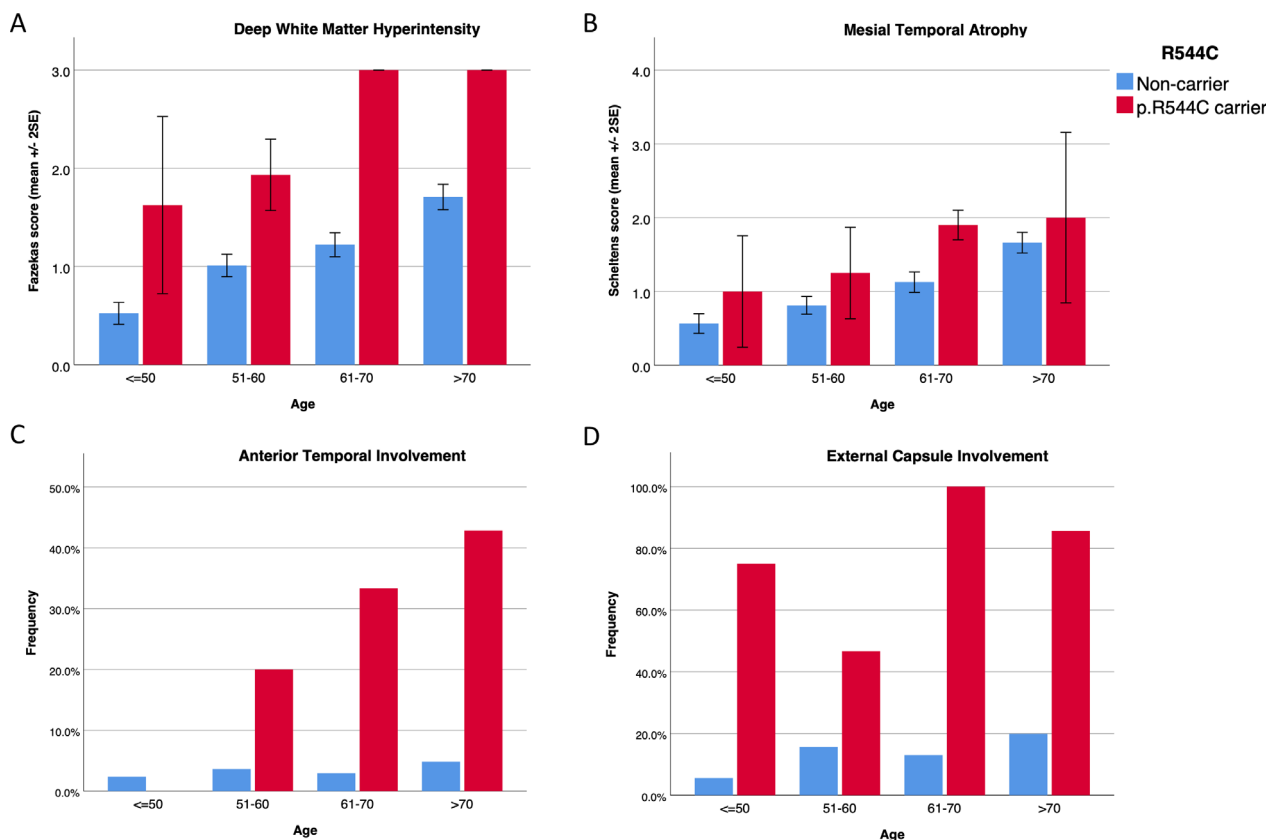


**Figure 2.** Imaging characteristics between subjects with and without *NOTCH3* p.R544C mutation according to age stratum. (A) White matter hyperintensity at deep white matter was more advanced in p.R544C mutation carriers, and was associated with advanced age. (B) Mesial temporal atrophy was associated with both advanced age and the p.R544C mutation status. (C) White matter lesions involving the anterior temporal pole was more frequent in p.R544C mutation carriers, and the frequency increased with age. (D) White matter lesions involving the external capsule was frequent in p.R544C mutation carriers regardless of age.

specificity, PPV, NPV, and accuracy were 0.750, 0.880, 0.131, 0.993, and 0.877, respectively (Table 5). The performance parameters of individual variables in the R544C screening score are summarized in supplementary table (Table S1). Although the excessive DWM hyperintensity for the age alone is associated with a sensitivity comparable to the full R544C screening score, the addition of the other four clinical parameters will increase the specificity to predict a positive p.R544C mutation test result from 0.823 to 0.880.

The demographic data and imaging characteristics of the validation cohort are shown in (Table S2). Six of the 235 subjects in the validation cohort harbored the *NOTCH3* p.R544C mutation. The ROC curve of the R544C screening score in the validation cohort is shown in (Fig. 3B). The area under the ROC curve was 0.957 (95% CI = 0.916-0.997). Using a cutoff score of 5, the sensitivity, specificity, PPV, NPV, and accuracy were 0.833, 0.895, 0.161, 0.996, and 0.894, respectively (Table 5).

The clinical usefulness of the R544C screening score was further shown by decision curve analysis (Figure 4). The decision curve analysis showed the net benefit of using the screening score to guide the *NOTCH3* p.R544C genetic testing over a range of risk threshold for genetic testing. Due to minimal risk and relatively low cost associated with genetic testing for a single-point mutation, we considered the clinically reasonable risk threshold to be less than 0.2 (i.e., number-needed-to-test more than 5). Over the relevant range of risk threshold, the R544C screening score provides a larger net benefit compared with stratifying patients by advanced DWM hyperintensity, external capsule involvement, or SVO stroke subtype alone.

### Discussion

We described the imaging characteristics of patients harboring the *NOTCH3* p.R544C mutation who presented with acute ischemic stroke/TIA. Based on the imaging

**Table 3.** Clinical and neuroimaging predictors for *NOTCH3* p.R544C mutation in subjects hospitalized for ischemic stroke or transient ischemic attack

Model <sup>†</sup>	Predictive factors	Odds ratio (95% CI)	P-value	AUC (95% CI)	Hosmer-Lemeshow test P-value
Model 1	Age of stroke	0.92 (0.881-0.969)	0.001	0.920 (0.881-0.958)	0.923
	TOAST_SVO	3.01 (1.19-7.64)	0.020		
	Stroke/TIA in siblings	3.42 (1.07-10.95)	0.038		
	External capsule involvement	4.18 (1.33-13.13)	0.014		
	Average DWM Fazekas score	4.35 (2.14-8.86)	<0.0005		
Model 2	Age of stroke_stratum		0.202	0.902 (0.843-0.960)	0.570
	Age of stroke <50	4.43 (1.06-18.53)	0.042		
	Age of stroke >50 and ≤60	1.35 (0.41-4.46)	0.627		
	Age of stroke >60 and ≤70	1.49 (0.37-5.96)	0.575		
	Age of stroke >70	(Reference group)			
	TOAST_SVO	2.98 (1.18-7.53)	0.021		
	Stroke/TIA in siblings	3.53 (1.01-11.71)	0.039		
	External capsule involvement	5.26 (1.78-15.57)	0.003		
	DWM Fazekas score significant for the age <sup>‡</sup>	11.46 (3.36-39.04)	<0.0005		
Model 3	Age of stroke before 50	3.50 (1.07-11.37)	0.038	0.900 (0.841-0.959)	0.602
	TOAST_SVO	2.99 (1.19-7.49)	0.019		
	Stroke/TIA in siblings	3.43 (1.05-11.18)	0.041		
	External capsule involvement	5.27 (1.80-15.47)	0.002		
	DWM Fazekas score significant for the age <sup>‡</sup>	10.99 (3.32-36.35)	<0.0005		

AUC, area under the ROC curve; TIA, transient ischemic attack; TOAST\_SVO, the small-artery occlusion stroke subtype; DWM, deep white matter.

<sup>†</sup>Models were built by multiple logistic regression. Model 1 was built by stepwise forward selection method with *P*-value < 0.05 for entry and *P*-value > 0.10 for removal from the model. Model 3 was used to develop the risk score.

<sup>‡</sup>WMH at deep white matter was considered significant if an average Fazekas score > 1 for subjects at or less than 60 years old, or an average Fazekas score > 2 for subjects aged more than 60 years.

and clinical characteristics, we developed an easily applicable screening score to guide p.R544C mutation screening in Taiwanese patients. Similar to the imaging findings in other *NOTCH3* pathogenic mutations,<sup>16,17</sup> we showed that the *NOTCH3* p.R544C mutation was associated with advanced WMH and white matter lesions involving the anterior temporal pole and the external capsule. It was suggested that WMH involving the anterior temporal pole may be more specific than WMH involving the external capsule for patients with CADASIL.<sup>18,19</sup> However, anterior temporal pole involvement was much less frequent for patients with CADASIL caused by the *NOTCH3* p.R544C mutation.<sup>4,8,20</sup> In our study, the frequency of anterior temporal pole involvement was only 22.2% for stroke patients harboring the p.R544C mutation, whereas the frequency of external capsule involvement was 69.4%. Another interesting finding was the modification effect of age on the extent of WMH in CADASIL patients. For patients harboring the *NOTCH3* p.R544C mutation, the frequency of anterior temporal pole involvement increased with age and reached up to 42.9% after the age of 70 years. On the other hand, the frequency of external capsule involvement was much higher in patients having the p.R544C mutation regardless of age. Therefore, WMH

involving the external capsule performed better in our scoring system.

In addition to white matter changes, we also measured the severity of mesial temporal atrophy by a visual rating scale. Previous morphometric MRI studies have shown that brain and cortical volumes are reduced<sup>21</sup> and cortical atrophy is associated with cognitive and functional decline in CADASIL patients.<sup>22,23</sup> To improve applicability in clinical practice, we used a simple visual rating method and still found significant mesial temporal atrophy in patients harboring the *NOTCH3* p.R544C mutation. However, when tested in the logistic regression model, the association between mesial temporal atrophy and the *NOTCH3* p.R544C mutation became nonsignificant after adjustment for WMH severity. One possible explanation is that cortical atrophy in CADASIL may be secondary to subcortical ischemic changes, such as the volume of lacunar lesions and subcortical infarcts.<sup>24,25</sup>

Pathogenic mutations for CADASIL can be located in any of exons 2-24 on the *NOTCH3* gene.<sup>2,26</sup> Because of the cost associated with genetic diagnosis for CADASIL, sagacious screening prior to genetic testing is greatly desired. Pescini *et al.* developed the CADASIL scale to guide *NOTCH3* genetic analysis by the use of eight

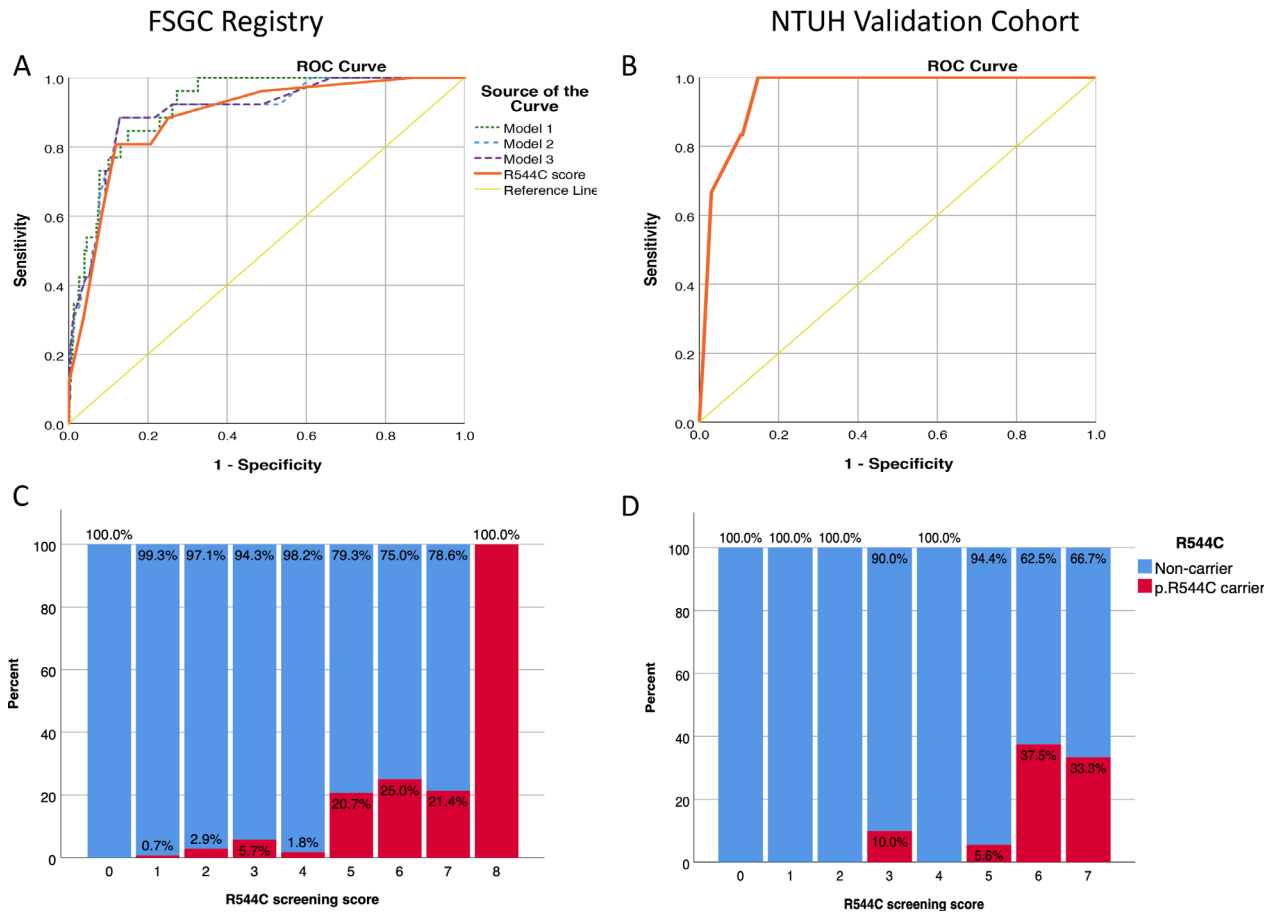


**Figure 3.** The receiver operating characteristic (ROC) curve and distribution of p.R544C mutation according to the R544C screening score in the FSGC registry (A,C) and the validation cohort (B,D).

**Table 4.** The R544C screening score

Score item	Subscore
Age of stroke onset $\leq$ 50 years	1
Small vessel occlusion (stroke subtype)	1
Family history of stroke or TIA in siblings	1
White matter lesions involving external capsule	2
Deep white matter WMH significant for the age	3
Fazekas score $>1$ for age $\leq 60$ , or	
Fazekas score $>2$ for age $>60$	

TIA, transient ischemic attack; WMH, white matter hyperintensity.

clinical and four imaging subscales.<sup>27</sup> The area under the ROC curve was 0.769, and the sensitivity and specificity for a cutoff core at 14 were 96.7% and 74.2%, respectively. However, the CADASIL scale was developed from patients with “clinical and neuroimaging features suggestive of CADASIL,” and the criteria for selecting patients to apply the scale were not specified. Liu *et al.* applied the CADASIL scale in 53 genetically confirmed Chinese

CADASIL patients, and the sensitivity was reduced to 64.1% (34/53).<sup>28</sup>

Bersano *et al.* developed a clinical algorithm to select patients from the Lombardia GeNetics of Stroke (GENS) project for further *NOTCH3* genetic analysis.<sup>29,30</sup> Patients admitted for subcortical lacunar infarct without obvious cause were recruited if they had either recurrent stroke or TIA, migraine with aura, dementia, major mood disorder, or a family history of the above symptoms. One hundred and twenty-eight patients were identified from approximately 11000 patients in the registry, and 16 (12.5%) of them had a pathogenic *NOTCH3* mutation. Because of the variable phenotype associated with different genotypes, none of the imaging-based pregenetic screening algorithms could be applied to all populations.<sup>16,17</sup>

In Taiwan, the predominance of the *NOTCH3* p.R544C mutation makes targeted genetic screening more efficient and practical. A major advantage of our R544C screening score is that it was developed for unselected patients who presented with acute ischemic cerebrovascular events in a

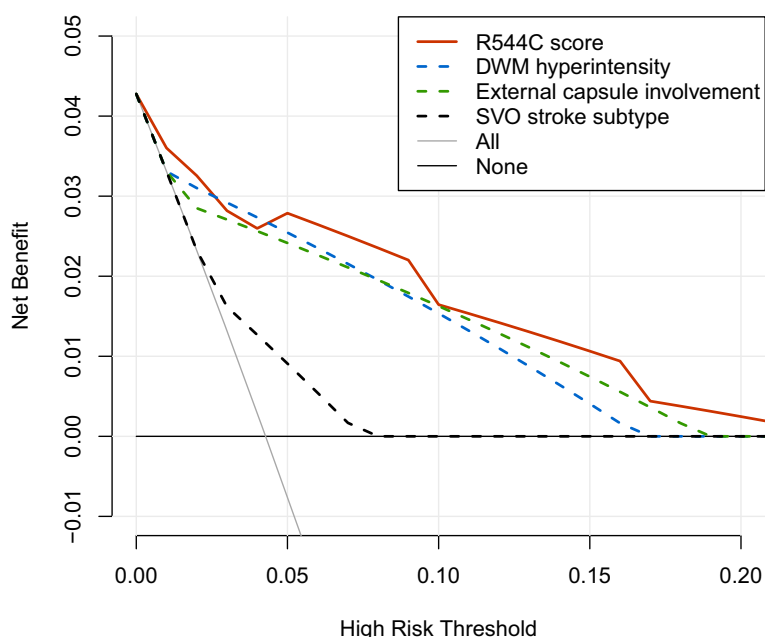


**Table 5.** Performance parameters of the R544C screening score.

Patient Population	Cutoff score	Sensitivity	Specificity	PPV <sup>†</sup>	NPV <sup>†</sup>	Accuracy	Youden's J statistic
FSGC stroke registry (N = 709)	1	1	0.128	0.027	1	0.149	0.128
	2	0.944	0.547	0.048	0.998	0.556	0.491
	3	0.833	0.749	0.074	0.995	0.751	0.582
	4	0.778	0.798	0.085	0.993	0.798	0.576
	5	0.75	0.88	0.131	0.993	0.877	0.63
	6	0.583	0.914	0.141	0.989	0.906	0.497
	7	0.25	0.967	0.155	0.982	0.950	0.217
	8	0.083	1	1	0.978	0.978	0.083
NTUH Validation cohort (N = 235)	5	0.833	0.895	0.161	0.996	0.894	

FSGC, Formosa Stroke Genetics Consortium; NPV, negative predictive value; NTUH, National Taiwan University Hospital; PPV, positive predictive value.

<sup>†</sup>PPV and NPV were calculated using the prevalence of positive p.R544C screening in the FSGC stroke registry (41/1734 = 2.36%).

**Figure 4.** Decision curve analysis for the R544C screening score compared with individual clinical or imaging parameters.

primary care setting. We only included five items in the screening score, and the scoring method is simple with good interrater reliability for the visual rating subscales. Using a cutoff score of 5, the positive predictive value was 0.131, and the negative predictive value was 0.993. The positive predictive value of the screening score was comparable to the algorithm developed by Bersano et al., whereas it was much more efficient since we only screened for a single-point mutation.

There were some limitations in this study. First, we did not sequence all the exons of the *NOTCH3* gene but only performed genotyping for the *NOTCH3* p.R544C mutation in the source population; thus, the R544C score may

not be applicable to detect other *NOTCH3* mutations. When applying the R544C screening score in clinical practice, one should be aware that even in Taiwan, about 30% of CADASIL is caused by *NOTCH3* mutations other than p.R544C and cannot be identified by p.R544C mutation screening. Subsequent sequencing for *NOTCH3* exons 2 to 24 should be performed for patients without the *NOTCH3* p.R544C mutation but having a high R544C screening score or having features suggestive of CADASIL, such as younger age of stroke, relevant family history, concurrent migraine and/or dementia, and white matter lesions involving the anterior temporal pole. Second, the number of subjects recruited in the validation

cohort was relatively small. Because of the low mutation prevalence, only six subjects in the validation cohort harbored the *NOTCH3* p.R544C mutation. Further application of the R544C screening score in larger populations in which p.R544C mutation accounts for the majority of CADASIL cases is needed to validate the generalizability of the score.

## Conclusion

For populations in which the *NOTCH3* p.R544C mutation accounts for the majority of CADASIL cases, the R544C screening score can efficiently guide p.R544C mutation detection in patients who present with acute cerebrovascular ischemic events. Targeted genetic testing for the *NOTCH3* p.R544C mutation may help identify cases at an early stage and be the foundation of further investigational trials for disease-modifying interventions.

## Author Contributions

YWC participated in the study design, conducted the statistical analysis, and drafted the manuscript. CHC participated in statistical analysis and helped in drafting the manuscript. All authors contributed to data acquisition. HYC conducted the *NOTCH3* p.R544C screening. SCT participated in concept formation, study design, and revised the draft manuscript. JSJ revised the draft paper. All authors reviewed and approved the final manuscript.

## Acknowledgments

We thank all the participants in the study. We thank the staff of Biotechnology R&D Center, National Taiwan University Hospital, Hsin-Chu Branch for their assistance in decision curve analysis. The study was funded by National Taiwan University Hospital, Hsin-Chu Branch, Taiwan (grant number: 108-HCH025).

## Conflict of Interest

The authors report no disclosures relevant to the manuscript.

## References

- Joutel A, Corpechot C, Ducros A, et al. Notch3 mutations in CADASIL, a hereditary adult-onset condition causing stroke and dementia. *Nature* 1996;383(6602):707–710.
- Rutten JW, Dauw HG, Gravesteyn G, et al. Archetypal *NOTCH3* mutations frequent in public exome: implications for CADASIL. *Ann Clin Transl Neurol* 2016;3(11):844–853.
- Joutel A, Vahedi K, Corpechot C, et al. Strong clustering and stereotyped nature of Notch3 mutations in CADASIL patients. *Lancet* 1997;350(9090):1511–1515.
- Liao YC, Hsiao CT, Fuh JL, et al. Characterization of CADASIL among the Han Chinese in Taiwan: Distinct Genotypic and Phenotypic Profiles. *PLoS One* 2015;10(8):e0136501.
- Tang SC, Chen YR, Chi NF, et al. Prevalence and clinical characteristics of stroke patients with p. R544C *NOTCH3* mutation in Taiwan. *Ann Clin Transl Neurol* 2019;6(1):121–128.
- Lee YC, Chung CP, Chang MH, et al. *NOTCH3* cysteine-altering variant is an important risk factor for stroke in the Taiwanese population. *Neurology* 2019.
- Choi JC, Song SK, Lee JS, et al. Diversity of stroke presentation in CADASIL: study from patients harboring the predominant *NOTCH3* mutation R544C. *J Stroke Cerebrovasc Dis.* 2013;22(2):126–131.
- Chen S, Ni W, Yin XZ, et al. Clinical features and mutation spectrum in Chinese patients with CADASIL: A multicenter retrospective study. *CNS Neurosci Ther* 2017;23(9):707–716.
- Hsieh YC, Seshadri S, Chung WT, et al. Association between genetic variant on chromosome 12p13 and stroke survival and recurrence: a one year prospective study in Taiwan. *J Biomed Sci.* 2012;3(19):1.
- Hsieh FI, Lien LM, Chen ST, et al. Get With the Guidelines-Stroke performance indicators: surveillance of stroke care in the Taiwan Stroke Registry: Get With the Guidelines-Stroke in Taiwan. *Circulation* 2010;122(11):1116–1123.
- Adams HP Jr, Bendixen BH, Kappelle LJ, et al. Classification of subtype of acute ischemic stroke. Definitions for use in a multicenter clinical trial. TOAST. Trial of Org 10172 in Acute Stroke Treatment. *Stroke* 1993;24(1):35–41.
- Fazekas F, Chawluk JB, Alavi A, et al. MR signal abnormalities at 1.5 T in Alzheimer's dementia and normal aging. *Am J Roentgenol* 1987;149(2):351–356.
- Ph Scheltens DL, Barkhof F, Huglo D, et al. Atrophy of medial temporal lobes on MRI in "probable" Alzheimer's disease and normal ageing: diagnostic value and neuropsychological correlates. *J Neurol Neurosurg Psychiatry* 1992;1992(55):967–972.
- Vickers AJ, Van Calster B, Steyerberg EW. Net benefit approaches to the evaluation of prediction models, molecular markers, and diagnostic tests. *BMJ* 2016;25(352):i6.
- Vickers AJ, van Calster B, Steyerberg EW. A simple, step-by-step guide to interpreting decision curve analysis. *Diagn Progn Res.* 2019;3:18.
- Schoemaker D, Quiroz YT, Torrico-Teave H, Arboleda-Velasquez JF. Clinical and research applications of

- magnetic resonance imaging in the study of CADASIL. *Neurosci Lett* 2019;17(698):173–179.
17. Jouvent E, Duering M, Chabriat H. Cerebral autosomal dominant arteriopathy with subcortical infarcts and leukoencephalopathy: lessons from neuroimaging. *Stroke* 2020;51(1):21–28.
  18. O'Sullivan M, Jarosz JM, Martin RJ, et al. MRI hyperintensities of the temporal lobe and external capsule in patients with CADASIL. *Neurology* 2001;56(5):628–634.
  19. Markus HS, Martin RJ, Simpson MA, et al. Diagnostic strategies in CADASIL. *Neurology* 2002;59(8):1134–1138.
  20. Chen CH, Tang SC, Cheng YW, et al. Detrimental effects of intracerebral haemorrhage on patients with CADASIL harbouring NOTCH3 R544C mutation. *J Neurol Neurosurg Psychiatry* 2019;90(7):841–843.
  21. Stromillo ML, Dotti MT, Battaglini M, et al. Structural and metabolic brain abnormalities in preclinical cerebral autosomal dominant arteriopathy with subcortical infarcts and leukoencephalopathy. *J Neurol Neurosurg Psychiatry* 2009;80(1):41–47.
  22. Peters N, Holtmannspotter M, Opherck C, et al. Brain volume changes in CADASIL: a serial MRI study in pure subcortical ischemic vascular disease. *Neurology* 2006;66(10):1517–1522.
  23. Jouvent E, Mangin JF, Porcher R, et al. Cortical changes in cerebral small vessel diseases: a 3D MRI study of cortical morphology in CADASIL. *Brain* 2008;131(Pt 8):2201–2208.
  24. Duering M, Righart R, Csanadi E, et al. Incident subcortical infarcts induce focal thinning in connected cortical regions. *Neurology* 2012;79(20):2025–2028.
  25. Jouvent E, Mangin JF, Duchesnay E, et al. Longitudinal changes of cortical morphology in CADASIL. *Neurobiol Aging* 2012;33(5):1002.e29–1002.e36.
  26. Chabriat H, Joutel A, Dichgans M, et al. Cadasil. *Lancet Neurol* 2009;8(7):643–653.
  27. Pescini F, Nannucci S, Bertaccini B, et al. The cerebral autosomal-dominant arteriopathy with subcortical infarcts and leukoencephalopathy (CADASIL) scale: a screening tool to select patients for NOTCH3 gene analysis. *Stroke* 2012;43(11):2871–2876.
  28. Liu X, Zuo Y, Sun W, et al. The genetic spectrum and the evaluation of CADASIL screening scale in Chinese patients with NOTCH3 mutations. *J Neurol Sci* 2015;354(1-2):63–69.
  29. Bersano A, Markus HS, Quagliani S, et al. clinical pre-genetic screening for stroke monogenic diseases: results from Lombardia GENS Registry. *Stroke* 2016;47(7):1702–1709.
  30. Bersano A, Bedini G, Markus HS, et al. The role of clinical and neuroimaging features in the diagnosis of CADASIL. *J Neurol* 2018;265(12):2934–2943.

## Supporting Information

Additional supporting information may be found online in the Supporting Information section at the end of the article.

**Table S1.** Performance parameters of individual variables in the R544C screening score.

**Table S2.** Demographics and imaging characteristics of the validation cohort.